

Fluorescence studies on the microenvironments of proteins in CO₂-expanded reverse micellar solutions

Jing Chen, Jianling Zhang, Yishi Wu, Buxing Han*, Dongxia Liu,
Zhonghao Li, Junchun Li, Xicheng Ai

Center for Molecular Sciences, Institute of Chemistry, Chinese Academy of Sciences, Beijing 100080, China

Received 25 January 2005; received in revised form 1 March 2005; accepted 1 November 2005

Abstract

The effect of compressed CO₂ on the microenvironment of the two proteins (cytochrome *c* and RNase A) in sodium bis(2-ethylhexyl)sulfosuccinate (AOT) reverse micelles was investigated using high-pressure steady-state fluorescence and time-resolved fluorescence. It is found that RNase A can shift from the water core to the interface of the reverse micellar cores as CO₂ is dissolved, while cytochrome *c* maintains at the interface of the micellar core. As the pressure reaches to a high enough value, the proteins can be precipitated from the reverse micelle, which has been detected by high-pressure UV–vis technique. The results show that cytochrome *c* was easier to be precipitated from the reverse micellar solution by CO₂ than RNase A. The possible reasons for these behaviors were discussed based on the changes of the microenvironment of the two proteins, which could be tuned by the dissolution of compressed CO₂.

© 2005 Elsevier B.V. All rights reserved.

Keywords: Fluorescence studies; RNase A; Cytochrome *c*

1. Introduction

Many kinds of reverse micelles are able to solubilize fairly large amount of water and hydrophilic molecules, such as proteins. The interest in these protein-containing micellar systems lies in biotechnological applications, in the mimicking of biological structures, and in the contribution to basic problems of structural biochemistry in particular to that part of biochemistry concerned with the relationship between environment and conformation/activity of functional biopolymers [1–7]. Some properties of protein-containing reverse micelles have been studied by spectroscopic measurements, such as CD [8,9], Raman [10] and fluorescence [11].

The properties of biomolecules in reverse micelles can be studied by fluorescence because different fluorophores like indole, tryptophan and tyrosine residues are sensitive to the physicochemical properties of their environment [12–15]. Steady-state fluorescence can reflect the influence of microviscosity, micropolarity and rigidity within the water pool on

biomolecules in reverse micelles [16]. Time-resolved fluorescence studies of proteins enable us to better understand how proteins behave in their native form or when sequestered within the water cores of reverse micelles [11,17–23].

It is known that compressed CO₂ can dissolve in many organic solvents, which results in considerable change in the solvent power of the solvents. Thus, changing the pressure can control the property of the liquid solvents, and separation of the gas and the liquid solvent can be achieved easily by depression. This principle has been used in extraction and fractionation, recrystallization of chemicals, and preparation of nanoparticles [24–28].

Dissolution of compressed CO₂ in the reverse micellar solution may adjust the properties of reverse micelles continuously. Our recent research demonstrated that the microenvironment of the water core in the reverse micelles, such as the polarity, ionic strength and pH value, could be tuned by the pressure of CO₂ [29], and the precipitation of inorganic nanoparticles in the reverse micelles were achieved at suitable pressure [30,31]. The application of compressed CO₂ into the protein-containing reverse micelles has also shown to be an interesting area. Zhang et al. have studied the recovery of proteins in reverse micelle by compressed CO₂, and pure and dry protein

* Corresponding author. Tel.: +86 10 62562821; fax: +86 10 62559373.
E-mail address: Hanbx@iccas.ac.cn (B. Han).

particles were obtained [32]. In our previous work, we have studied the effect of compressed CO₂ on microenvironment of protein (trypsin) in the reverse micelles using UV and FT-IR spectroscopy and precipitation of the protein [33]. It was found that dissolution of CO₂ in the micellar solution could cause the changes of the microenvironment of the proteins in the reverse micelles.

The fluorescence of proteins is a very sensitive indicator of the microenvironment of the tryptophan residues. In general, the wavelength of maximum emission should exhibit a blue shift as the polarity of the tryptophan environment decreases [16,34,35]. In present work, we further our studies on the CO₂-expanded protein-containing reverse micellar system using steady-state fluorescence and time-resolved fluorescence and UV. Two proteins, RNase A and cytochrome *c*, were selected. The fluorescence emission of RNase A arises from the six tyrosine residues [36,37]. And the fluorescence emission of cytochrome *c* is from one tryptophan residue [38]. The former is located in the water core of the reverse micelles and the latter is located at the interface of the micellar cores [39] in the absence of CO₂. RNase A contains 19 of the 20 natural amino acids, lacking only tryptophan. Three of the six tyrosines in RNase A are known to be buried in the native molecule whereas the other three are located on the protein surface. The enzyme is cross-linked by four disulfide bonds and the predominant elements of secondary structure are a long four-stranded antiparallel β -sheet and three short α -helices. The overall shape of the enzyme resembles that of a kidney. The stability of RNase A is legendary. RNase A has no change of secondary structure in the high w_0 (water-to-surfactant molar ratio) reverse micelles [40,37]. Cytochrome is strongly associated with the inner mitochondrial membrane in vivo. This protein contains 19 lysine residues, which can be expected to make electrostatic interaction with anionic surfactants. Most of these residues are distributed on the two flanks of the protein molecule. However, this protein does not show a drastic change of secondary structure upon the incorporation into the reverse micelles and the addition of sodium dodecyl sulphate (SDS) to the aqueous protein solutions [41]. The effect of the compressed CO₂ on the microenvironment and micro-behavior of the proteins (cytochrome *c* and RNase A) in the reverse micelles were discussed. The investigations provide fundamental understanding for such systems and necessary information of the related potential applications.

2. Experimental

2.1. Materials

Cytochrome *c* (bovine, $M_w = 12,310$, PI = 10.0) was purchased from DongZhiKai Biotechnology Co. in Beijing and RNase A (bovine, $M_w = 13,690$, PI = 7.8) from Sigma. The two proteins were used directly without further purification. AOT was purchased from sigma and used after drying under vacuum for at least 2 h. *n*-Decane was purchased from Tianjin Wendaixigui Chemical Co. CO₂ (99.995%) was provided by Beijing Analytical Instrument Factory.

2.2. Preparation of reverse micellar solution

Concentrated stock solution of protein (150 mg/ml) was prepared in twice distilled water. A suitable amount of protein aqueous solution was injected into the AOT/decane solution, then appropriate amounts of water was subsequently added to achieve desired w_0 (water-to-surfactant molar ratio). The solution was shaken until it was transparent. The molar ratio of fluorophore to surfactant was carefully chosen to give an optimum signal-to-noise ratio with minimal perturbation to the micellar organization and negligible interprobe interactions. The final protein concentration in reverse micellar solution after expanded by CO₂ was 0.5 mg/ml, and the concentration of AOT was 100 mmol/l in all cases. The final molar ratio of protein to surfactant is 1:2462 for cytochrome *c* and 1:2738 for RNase A, respectively. At such a low fluorophore to surfactant molar ratio, the number of protein molecule in each reverse micelle would be no more than one on an average, which rules out molecule aggregation effects [42,43].

2.3. Phase behavior of reverse micellar solution in CO₂

The apparatus used to study the expansion curves and the cloud point pressure of the solution was the same as that used previously [28]. In the expansion experiment, suitable amount of reverse micellar solution was added into the view cell. The temperature of the water bath was controlled by a HAAKE D3 digital controller, and the accuracy of the temperature measurement was ± 0.1 °C. After the thermal equilibrium had been reached, CO₂ was charged into the cell to a suitable pressure. A magnetic stirrer was used to enhance the mixing of CO₂ and reverse micellar solution. The pressure and the volume at equilibrium condition were recorded. More CO₂ was added and the volume of the liquid phase at another pressure was determined. The volume expansion coefficients were calculated on the basis of the liquid volumes before and after dissolution of CO₂.

2.4. UV measurements

A UV spectrophotometer (TU-1201, Beijing Purkin General Instrument Co., Ltd.) was used to examine the precipitation of the proteins from the reverse micelles at different pressures. The UV sample cell was the same as that used previously [44], and the maximal operating pressure and temperature of the cell is about 20 MPa and about 60 °C, respectively. The optical path length and the volume of the sample cell were 1.12 cm and 1.76 ml, respectively. In the experiments, suitable amount of protein-containing reverse micellar solution was loaded into the cell. The temperature of the cell was maintained at 298.2 K. After the thermal equilibrium was reached, CO₂ was charged into the sample cell until the cell was full. The UV spectrum of solution was obtained by repeated scans until it was unchanged. The concentration of the protein in the solution was known from the absorption maximum.

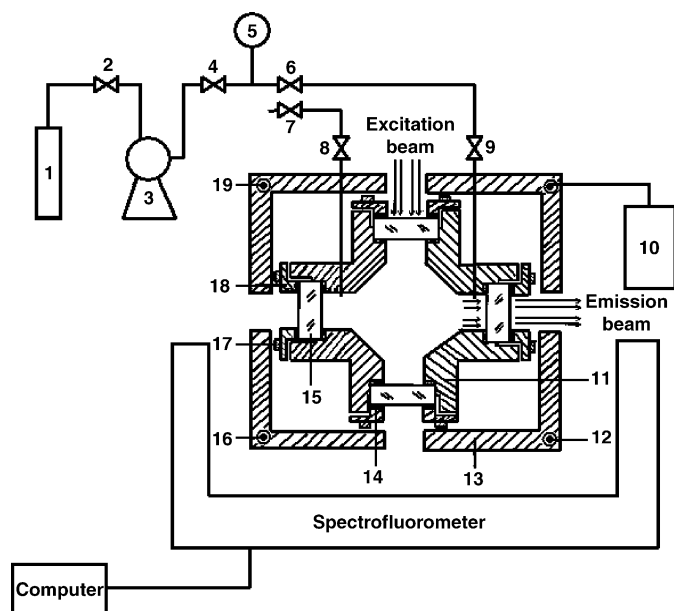


Fig. 1. Schematic diagram of the apparatus for high-pressure fluorescence study. (1) Gas cylinder; (3) high-pressure pump; (5) pressure gauge; (10) temperature controller; (11) stainless-steel body; (12, 16, 19) electric heaters; (13) outside heating box; (14) Teflon gasket; (15) quartz window; (17, 18) nuts; (2, 4, 6–9) valves.

2.5. Steady-state fluorescence measurements

Steady-state fluorescence measurements were performed with a F-2500 spectrofluorometer (Hitachi, Ltd., Tokyo, Japan) using a high-pressure fluorescent cell shown in Fig. 1. The volume of the sample cell was 8.44 ml. In the experiment, a suitable amount of protein-containing reverse micellar solution was charged into the cell. The temperature of the cell was maintained at 298.2 K. Then CO₂ was charged until the sample cell was full. The fluorescence spectrum of solution was obtained after the thermal equilibrium was reached. The excited wavelength is 280 nm and the excitation and emission slits with a nominal band-pass of 5 nm were used for all measurements. For all the fluorescence measurements, the pressure was controlled to be lower than the precipitation pressure of proteins in order to avoid the deposition of proteins from the reverse micelles.

A shift in the wavelength of maximum fluorescence emission toward higher wavelengths, caused by a shift in the excitation wavelength toward the red edge of absorption band, is termed as red edge excitation shift (REES). To gain some information about the relative rates of solvent relaxation dynamics, we introduced REES technique into the CO₂-expanded reverse micellar system. This effect is mostly observed with polar fluorophores in motionally restricted media, such as very viscous solutions or condensed phases where the dipolar relaxation time for the solvent shell around a fluorophore is comparable to or longer than its fluorescence lifetime [45–48]. REES arises from slow rates of solvent relaxation (reorientation) around an excited state fluorophore (as compared to the fluorescence lifetime), which is a function of the motional restriction imposed on the solvent molecules in the immediate vicinity of the fluorophore. Utilizing

this approach, it becomes possible to probe the mobility parameters of the environment itself using the fluorophore merely as a reporter group [42,49,50].

2.6. Time-resolved fluorescence measurements

The sample cell for the experimental procedures were the same as that used in steady-state fluorescence measurements. The temperature of the cell was maintained at 298.2 K and the excited wavelength is 280 nm for all measurements. Fluorescence lifetimes were calculated from time-resolved fluorescence intensity decays using a photo-counting streak camera (C2909, Hamamatsu Photonics Co., Japan). This machine uses a femto-second laser source running at 1 KHz. The laser's output wavelength could be set to the desired excitation with OPA (OPA-800CF, Spectra Physics, USA). To optimize the signal-to-noise ratio, 10,000 photon counts were collected in the peak channel. All experiments were performed using excitation and emission slits with a nominal band-pass of 4 and 2 nm. This arrangement also prevented any prolonged exposure of the sample to the excitation beam, thereby avoiding any possible optical damage of the fluorophore. The data detected by digital camera (C4742-95, Hamamatsu Photonics Co.) was transferred to an IBM PC for analysis. Intensity decay curves so obtained were fitted as a sum of exponential terms [42,50].

$$F(t) = \sum \alpha_i \exp\left(\frac{-t}{\tau_i}\right), \quad (1)$$

where α_i is a pre-exponential factor representing the fractional contribution to the time-resolved decay of the component with lifetime τ_i . The decay parameters were recovered using a nonlinear least squares iterative fitting procedure based on Matlab5.3 (Mathworks). The program also included statistical and plotting subroutine packages. The goodness of the fit of a given set of observed data and the chosen function were evaluated by the weighted residuals. A fit was considered acceptable when plots of the weighted residues showed random deviation about zero. Mean lifetime (τ) for bi-exponential decays of fluorescence were calculated from the lifetimes and pre-exponential factors using the following equation [42,50]:

$$\langle \tau \rangle = \frac{\alpha_1 \tau_1^2 + \alpha_2 \tau_2^2}{\alpha_1 \tau_1 + \alpha_2 \tau_2}. \quad (2)$$

3. Results and discussion

3.1. Phase behavior investigation of the reverse micelles in CO₂

The solution is expanded after dissolution of CO₂. The volume expansion coefficient ΔV ($\Delta V = (V - V_0)/V_0$, where V and V_0 are the volumes of the CO₂-saturated and CO₂-free reverse micellar solution) of the solution at different pressures is a very important parameter in the experiments. Fig. 2 shows the volume expansion curves of the solution ([AOT] = 100 mmol/l, $w_0 = 2.5, 5, 10$) versus the pressure at 298.2 K obtained in this work. The volume expansion coefficient increases with pressure.

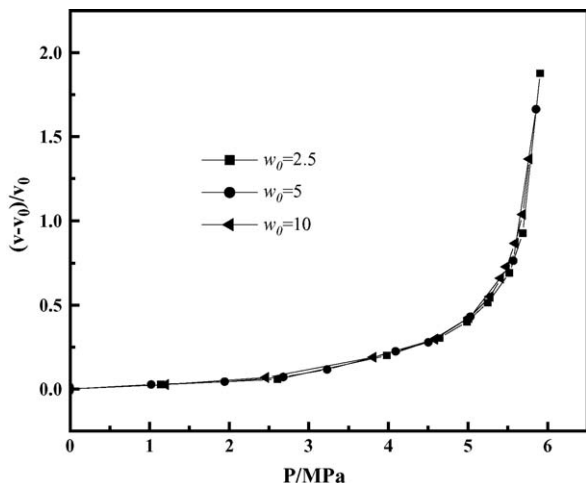


Fig. 2. The volume expansion curves of the water/AOT/decane reverse micellar solution ($[AOT] = 100 \text{ mmol/l}$, $w_0 = 2.5, 5, 10$) vs. the pressure at 298.2 K.

We also studied the effects of protein concentrations (from 0 to 0.5 mg/ml) on the volume expansion. The results indicated that the effect of w_0 and protein concentration on the ΔV were not considerable. The determined volume expansion allowed us to determine how much CO_2 -free reverse micellar solutions should be loaded into sample cell for the UV and fluorescence investigations. The solution became cloudy at the cloud point pressure, where the surfactant began to precipitate. The cloud point pressures of the AOT/water/decane micellar solutions at $w_0 = 2.5, 5$ and 10 determined are 5.91, 5.86 and 5.77 MPa at 298.2 K, with a precision of ± 0.03 MPa.

3.2. Precipitation of proteins in the presence of CO_2

In the absence of CO_2 , precipitation of the proteins in the reverse micelles did not occur. However, the proteins were precipitated with the dissolution of CO_2 in the solution. In this work we determined the precipitation of the two proteins from the reverse micelles at different CO_2 pressures using UV method. Cytochrome *c* and RNase A in the solution showed maximum absorption at 276 and 273 nm, respectively, and the absorbance was linear function of their concentration in the range of 0–0.5 mg/ml. As examples, Fig. 3 shows the precipitation of cytochrome *c* from CO_2 -expanded reverse micellar solution at different w_0 and that of RNase A at $w_0 = 10$. As CO_2 pressure reaches to a high enough value, the protein in the reverse micelles begins to precipitate, and the precipitation percentage increases gradually with the increase of pressure. Moreover, it can also be seen from Fig. 3 that the precipitation of cytochrome *c* is easier at higher w_0 . This is maybe due to the fact that the microenvironment of the proteins in the water core is stricter at low w_0 [51]. Fig. 3 also demonstrates that cytochrome *c* begins to precipitate at the lower pressure than RNase A. According to the study of Petit et al. [39], cytochrome *c* is located at the surface of micellar core, while RNase A is located in the water core, which is due to the stronger hydrophilic properties of RNase A than that of cytochrome *c*. Even if RNase A is loaded in the interface of the reverse micelle, the hydrophilic properties of

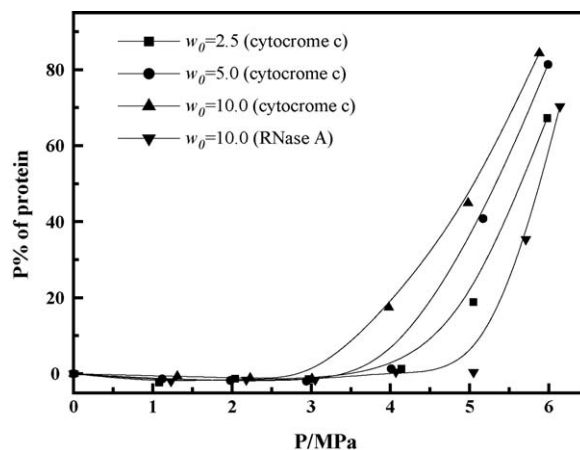


Fig. 3. Effect of pressure on precipitation percentage ($P\%$) of cytochrome *c* and RNase A in the reverse micellar solution at 298.2 K.

RNase A should be still stronger than that of cytochrome *c* in the interface. Thus, it is easier for cytochrome *c* to precipitate from reverse micelles than RNase A.

3.3. Steady-state fluorescence of proteins in CO_2 -expanded reverse micellar solution

The fluorescence spectra of cytochrome *c* in CO_2 -free reverse micelles and water are shown in Fig. 4. The maximum emission wavelength of the protein in reverse micelles has a blue shift in comparison to that in water reflecting a decrease in the average polarity near the emitting tryptophan residue, which is in good agreement with that reported by other authors [17,34]. Consequently, it is agreement that the polarity of the water core is lower than that of the aqueous solution. The center of gravity of the protein fluorescence has a mild blue shift as w_0 increases from 2.5 to 10.0, but the wavelength of maximum emission has no obvious variation. This is maybe due to the fact that cytochrome *c* exists at the interface of reverse micelles [39,41], the polarity of the interface of the reverse micelle should not change remarkably as the w_0 changes. Therefore, the wavelength of maximum

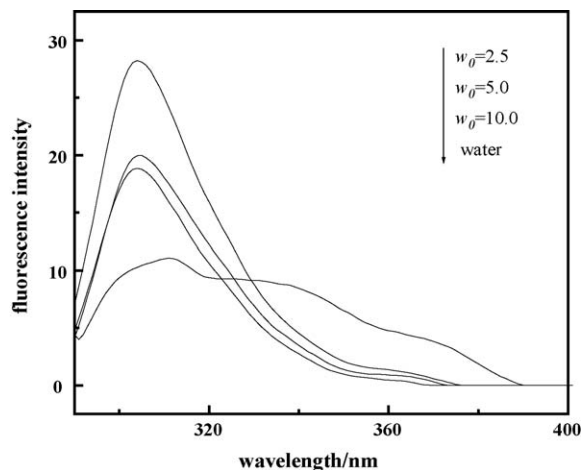


Fig. 4. Fluorescence spectra of cytochrome *c* in CO_2 -free reverse micellar solution and water at 298.2 K.

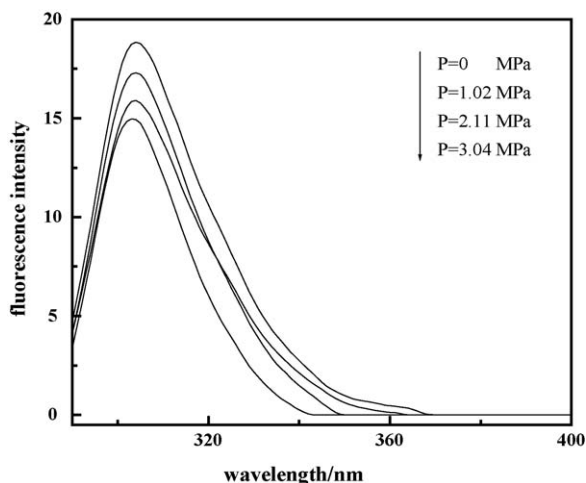


Fig. 5. Fluorescence spectra of cytochrome *c* in reverse micellar solution at $w_0 = 10.0$ as a function of pressure at 298.2 K.

emission of cytochrome *c* in the interface has no change considerably with w_0 .

Fig. 5 shows the fluorescence spectra of cytochrome *c* in reverse micelles ($w_0 = 10$) at different pressures, and the corresponding fluorescence emission maximum and intensity are listed in Table 1. As we can see, the fluorescence intensity of cytochrome *c* decreases with the increase of pressure. This result indicates that the fluorescence quenching of cytochrome *c* increases after CO₂ is charged. It is known that proton has great effect on the quenching of fluorophore [52]. Our previous study demonstrated that CO₂ could dissolve in the water core and hydrolyze ($\text{CO}_2 + \text{H}_2\text{O} = \text{HCO}_3^- + \text{H}^+$) [29], and pH value of the micellar cores decreased with the increase of CO₂ pressure (e.g. the pH value of the water core decreases from about 7.0 to about 3.6 as the pressure of CO₂ increases from 0 to about 4.5 MPa at $w_0 = 10$). Therefore, the concentration of proton increases as CO₂ is charged, resulting in the fluorescence quenching of fluorophore.

Table 1 also shows fluorescence emission maximum and intensity of cytochrome *c* and RNase A in AOT/decane reverse micelles at different w_0 as a function of pressure. As we can see, there is almost no shift in the wavelength of maximum emission for cytochrome *c* in all cases, while an obvious blue shift in the wavelength of maximum emission of RNase A can be observed as the pressure of CO₂ increase from 0 to 1.04 MPa, and there is no obvious shift in the wavelength of maximum emission from

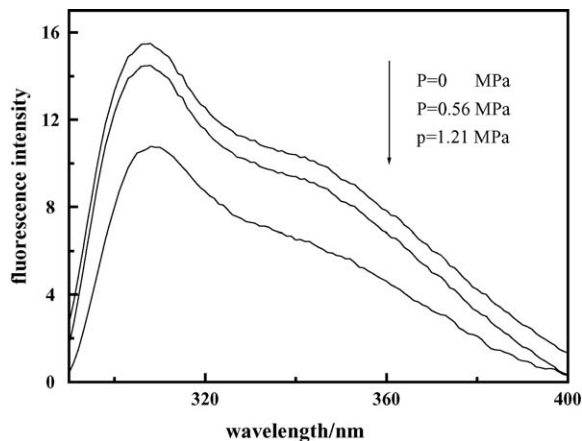


Fig. 6. Fluorescence spectra of RNase A in aqueous solution as a function of pressure at 298.2 K.

1.04 to 4.01 MPa. And as shown in Fig. 6 the wavelength of maximum emission of RNase A in aqueous solution has no changes with the increasing of CO₂ pressure. This indicates that RNase A has no conformation change with CO₂ (pH). It is known that RNase A can shift from the water core to the surface of reverse micelles as the pH of water core decreases because for such proteins the electrostatic interactions are more efficient than the hydrophilic character of the protein [39]. This maybe can be explained by the following reason [53]: at pH values around the isoelectric point (pI 7.8) of RNase A, the protein in neuter reverse micelles will have a little positive charge so the interaction between the protein and the AOT head groups is weak and the protein stay in the water core; while at pH values below its isoelectric point (pI 7.8), the protein in acidic reverse micelles will have a net positive charge so the interaction between the protein and the AOT head group become strong and the protein shift from the water core to the surface of reverse micelles. Thus, it is reasonable to expect that the location of RNase A is varied by the dissolution of CO₂, i.e. it migrates from the water pool to the interface of the reverse micelle. However, for cytochrome *c*, it maintains at the interface of the reverse micelle during the loading of CO₂. The water near the interface is bonded water of which properties are different from the free water of the water core [29], and so the polarity of interface should still be smaller than that of water core. So the wavelength of maximum emission for cytochrome *c* has no obvious shift because the protein is located in the interface of the reverse micelles without obvious polarity changes, and the wavelength of maximum emission for

Table 1
Fluorescence emission maxima (λ_{max}) and intensity (*I*) of cytochrome *c* and RNase A in AOT/decane reverse micelles at different w_0 and pressures (298.2 K)

<i>P</i> (MPa)	Cyt($w_0 = 2.5$)		Cyt($w_0 = 5.0$)		Cyt($w_0 = 10.0$)		RNase A($w_0 = 10.0$)	
	λ_{max} (nm)	<i>I</i>						
0	304.0	28.24	304.5	19.99	304.0	18.82	314.0	123.2
1.04	304.0	19.44	304.0	17.35	304.0	17.26	308.0	121.5
2.02	303.5	19.50	303.0	16.85	304.0	15.86	307.5	118.3
3.08	303.5	18.91	303.0	16.13	303.5	14.97	307.0	111.4
4.01	303.5	17.83	303.0	9.94			306.5	102

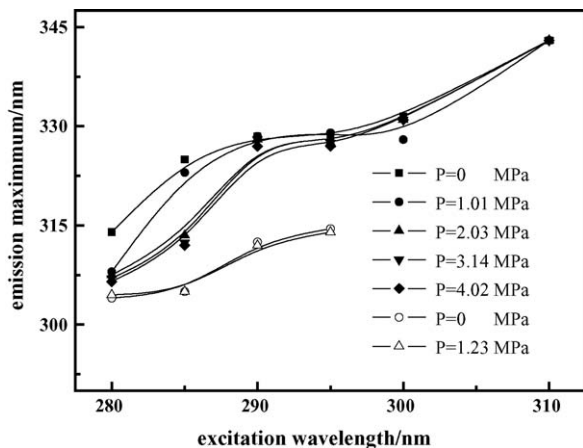


Fig. 7. Effect of changing excitation wavelength on the maximum wavelength of emission of RNase A (solid symbols) and cytochrome *c* (hollow symbols) in reverse micelles of AOT in decane with $w_0 = 10$ at different pressures and 298.2 K.

RNase has a big change because the protein shifts from the water core to the interface of the reverse micelles with a large polarity changes.

3.4. REES

As a useful fluorescence technique, REES can provide information about solvent relaxation dynamics. The REES value represents the extent of probe restricted, i.e. the higher the REES value is, the more the probe is restricted [42]. Fig. 7 shows the effect of changing excitation wavelength on the wavelength of maximum emission of RNase A and cytochrome *c* in the reverse micelles ($w_0 = 10$) at different pressures. As the excitation wavelength is changed from 280 to 310 nm, the emission maxima of RNase A loaded in reverse micelles display shift toward longer wavelengths in all cases. The emission maxima shift from 314 to 343 nm (in absence of CO_2), 308 to 343 nm ($P = 1.14$ MPa), 307.5 to 343 nm ($P = 2.05$ MPa), 307 to 343 nm ($P = 3.09$ MPa) and 306.5 to 343 nm ($P = 4.01$ MPa). Such dependence of the emission spectra on the excitation wavelength is characteristic of the red edge effect and indicates that RNase A is localized in a motionally restricted environment that offers considerable resistance to solvent reorientation in the excited state. In other words, the microenvironment of RNase A in the water core is changed considerably as CO_2 is charged, and the motion of RNase A in the micellar core is more restricted. This is consistent with the migration of RNase A from the water pool to the interface. The emission maxima of cytochrome *c* in the reverse micelles also display shift toward longer wavelengths in all cases, while cytochrome *c* has no obvious change in REES. This confirms that RNase A has a shift from water core to interface, while cytochrome *c* maintains in the interface of reverse micelle when CO_2 is charged.

3.5. Time-resolved fluorescence of proteins

Time-resolved fluorescence can provide further evidence for the changes of the environment of proteins [42,50]. As examples,

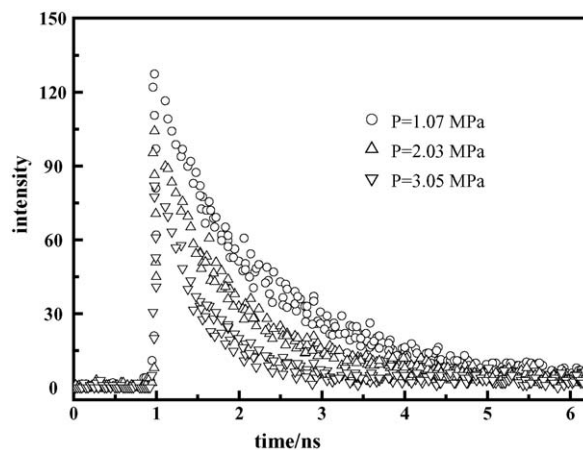


Fig. 8. Time-resolved fluorescence decay profiles for cytochrome *c* in reverse micelles ($w_0 = 10$) at different pressures and 298.2 K. The decay curves are best fitted to a sum of two exponentials.

Fig. 8 shows typical time-resolved fluorescence decay profiles for cytochrome *c* in reverse micelles ($w_0 = 10$) at different pressures. The decay curves are best fitted to a sum of two exponentials. As it can be seen, the fluorescence intensity decreases as pressure increases, which is similar to that of the steady-state fluorescence.

The analysis of the data (lifetime, τ_i , normalized amplitudes, α_i , and the mean lifetime, $\langle \tau \rangle$) for the double exponential decays of the two proteins yields the values listed in Table 2. The lifetime and the mean lifetime of cytochrome *c* and RNase A in the reverse micelles decrease with increasing pressure. The polarity of water core of reverse micelle can be increased with the hydrolyzing of CO_2 . This makes the decreasing of lifetimes and mean lifetimes for the two enzymes. Moreover, it is clear that the difference of lifetime of cytochrome *c* with and without CO_2 is smaller than that of RNase A. This is related to the fact that cytochrome *c* lies in a comparable strict environment because it exists at the interface of reverse micelles, while RNase A can shift from the water core to the interface, resulting in the large difference of lifetime with the dissolution of CO_2 . This is consistent with the steady-state fluorescence results.

Table 2

Lifetimes of cytochrome *c* and RNase A in AOT/decane reverse micelles ($w_0 = 10$) at different w_0 and pressures (298.2 K)

<i>P</i> (MPa)	α_1	τ_1 (ns)	α_2	τ_2 (ns)	$\langle \tau \rangle$ (ns)
(a) Cytochrome <i>c</i>					
0	0.63	0.52 ± 0.11	0.37	2.58 ± 0.51	1.28
1.07	0.59	0.46 ± 0.09	0.41	2.01 ± 0.34	1.10
2.03	0.50	0.22 ± 0.06	0.50	1.47 ± 0.16	0.84
3.05	0.67	0.40 ± 0.09	0.35	1.70 ± 0.42	0.83
(b) RNase A					
0	0.54	0.99 ± 0.41	0.46	4.64 ± 0.53	2.68
1.01	0.56	0.91 ± 0.32	0.44	4.32 ± 0.21	2.41
2.04	0.59	0.72 ± 0.22	0.41	4.17 ± 0.15	2.12
3.03	0.60	0.81 ± 0.36	0.40	3.65 ± 0.18	1.94
4.06	0.59	0.47 ± 0.11	0.41	3.22 ± 0.12	1.59

4. Conclusion

In this paper, the precipitation, microenvironment and micro-behavior of the proteins cytochrome *c* and RNase A in CO₂-expanded reverse micellar solutions were studied by high-pressure UV–vis spectra, steady-state and time-resolved fluorescence techniques, respectively. It is demonstrated that the dissolution of compressed CO₂ into the micellar solutions results in the migration of RNase A from the water pool to the interface of the micelle. And as the pressure reaches to a high enough value, both of these two proteins can be precipitated from the solutions, and the higher the pressure used, the more proteins could be precipitated. Thus, the compressed CO₂ and its pressure can be used as variables to tune the microenvironment, micro-behavior and precipitation of the proteins in reverse micelles.

Acknowledgements

The authors are grateful to the National Natural Science Foundation of China (20403021, 20133030).

References

- [1] B. Steinmann, H. Jäckle, P.L. Luisi, A comparative study of lysozyme conformation in various reverse micellar systems, *Biopolymers* 25 (1986) 1133.
- [2] S.M. Andrade, S.M.B. Costa, Structural changes of α -chymotrypsin in reverse micelles of AOT studied by steady state and transient state fluorescence spectroscopy, *J. Mol. Struct.* 565 (2001) 219.
- [3] V.N. Dorovskis-Taran, C. Veeger, A.J.W.G. Visser, Comparison of the dynamic structure of α -chymotrypsin in aqueous-solution and in reversed micelles by fluorescence active-site probing, *Eur. J. Biochem.* 211 (1993) 47.
- [4] P. Walde, Q.Q. Peng, N.W. Fadnavis, E. Battistel, P.L. Luisi, Structure and activity of trypsin in reverse micelles, *Eur. J. Biochem.* 173 (1988) 401.
- [5] P.D.J. Fletcher, R.B. Freedman, J. Mead, C. Oldfield, B.H. Robinson, Reactivity of α -chymotrypsin in water-oil microemulsions, *Colloids Surf.* 10 (1984) 193.
- [6] S. Barbaric, P.L. Luisi, Micellar solubilization of biopolymers in organic solvents. 5. Activity and conformation of α -chymotrypsin in isoctane-AOT reverse micelles, *J. Am. Chem. Soc.* 103 (1981) 4239.
- [7] H. Zhu, Y.X. Fan, N. Shi, J.M. Zhou, Activity and conformation changes of Chinese hamster dihydrofolate reductase in reverse micelles, *Arch. Biochem. Biophys.* 368 (1999) 61.
- [8] K. Takeda, K. Harada, K. Yamaguchi, Y. Moriyama, Conformational changes of bovine serum albumin in an aqueous solution of sodium bis(2-ethylhexyl) sulfosuccinate and in the reverse micelle of the same surfactant, *J. Colloid Interface Sci.* 164 (1994) 382.
- [9] K. Takeda, M. Shigeta, K. Aoki, Secondary structures of bovine serum albumin in anionic and cationic surfactant solutions, *J. Colloid Interface Sci.* 117 (1987) 120.
- [10] B.A. Bolton, J.A. Scherer, Raman spectra and water absorption of bovine serum albumin, *J. Phys. Chem.* 93 (1989) 7635.
- [11] J.S. Lundgren, M.P. Heitz, F.V. Bright, Dynamics of acrylodan-labeled bovine and human serum-albumin sequestered within aerosol-OT reverse micelles, *Anal. Chem.* 67 (1995) 3775.
- [12] M.R. Eftink, Y.W. Jia, D.N. Hu, C.A. Ghiron, Fluorescence studies with tryptophan analogs—excited-state interactions involving the side-chain amino group, *J. Phys. Chem.* 99 (1995) 5713.
- [13] D. Creed, The photophysics and photochemistry of the near-UV absorbing amino acids—I. Tryptophan and its simple derivatives, *Photochem. Photobiol.* 39 (1984) 537.
- [14] J.M. Beechem, L. Brand, Time-resolved fluorescence of proteins, *Annu. Rev. Biochem.* 54 (1985) 43.
- [15] R. Swaminathan, G. Krishnamorthy, N. Periasamy, Similarity of fluorescence lifetime distributions for single tryptophan proteins in the random coil state, *Biophys. J.* 67 (1994) 2013.
- [16] S.M. Andrade, S.M.B. Costa, The location of tryptophan, *N*-acetyltryptophan and α -chymotrypsin in reverse micelles of AOT: a fluorescence study, *Photochem. Photobiol.* 72 (4) (2000) 444.
- [17] P. Marzola, E. Gratton, Hydration and protein dynamics-frequency-domain fluorescence spectroscopy on proteins in reverse micelles, *J. Phys. Chem.* 95 (1991) 9488.
- [18] P. Marzola, C. Pinzoni, A. Veracini, Spin-labeling study of human serum-albumin in reverse micelles, *Langmuir* 7 (1991) 238.
- [19] J.D. Jordan, R.A. Dunbar, F.V. Bright, Dynamics of acrylodan-labeled bovine and human serum-albumin entrapped in a sol-gel-derived biogel, *Anal. Chem.* 67 (1995) 2436.
- [20] C. Reichardt, Solvatochromic dyes as solvent polarity indicators, *Chem. Rev.* 94 (1994) 2319.
- [21] R. Wang, S. Sun, E.J. Bekos, F.V. Bright, Dynamics surrounding cysteine 34 in native, chemically denatured, and silica-adsorbed bovine serum-albumin, *Anal. Chem.* 67 (1995) 149.
- [22] J.S. Lundgren, F.V. Bright, Effects of surfactants on the dynamical behavior of acrylodan-labeled bovine serum albumin, *J. Phys. Chem.* 100 (1996) 8580.
- [23] D.W. Pierce, S.G. Boxer, Dielectric-relaxation in a protein matrix, *J. Phys. Chem.* 96 (1992) 5560.
- [24] M.A. Winters, D.Z. Frankel, P.G. Debenedetti, J. Carey, M. Devaney, T.M. Przybycien, Protein purification with vapor-phase carbon dioxide, *Biotechnol. Bioeng.* 62 (1999) 247.
- [25] F. Favari, A. Bertuccio, N. Elvassore, M. Fermeglia, Multiphase multi-component equilibria for mixtures containing polymers by the perturbation theory, *Chem. Eng. Sci.* 55 (2000) 2379.
- [26] M. Muller, U. Meier, A. Kessler, M. Mazzotti, *Ind. Eng. Chem. Res.* 39 (2000) 2260.
- [27] P. Chattopadhyay, R.B. Gupta, *Ind. Eng. Chem. Res.* 39 (2000) 2281.
- [28] D. Li, Z.M. Liu, G.Y. Yang, B.X. Han, H.K. Yan, Phase equilibria of CO₂-PET-phenol system and generation of PET powders by supercritical CO₂ anti-solvent, *Polymer* 41 (2000) 5707.
- [29] D.X. Liu, J.L. Zhang, B.X. Han, J.F. Fan, T.C. Mu, Z.M. Liu, W.Z. Wu, J. Chen, Effect of compressed CO₂ on the properties of AOT reverse micelles studied by spectroscopy and phase behavior, *J. Chem. Phys.* 119 (9) (2003) 4873.
- [30] J.L. Zhang, B.X. Han, J.C. Liu, X.G. Zhang, J. He, Z.M. Liu, A new method to recover the nanoparticles from reverse micelles: recovery of ZnS nanoparticles synthesized in reverse micelles by compressed CO₂, *Chem. Commun.* (2001) 2724.
- [31] J.L. Zhang, B.X. Han, J.C. Liu, Recovery of silver nanoparticles synthesized in AOT/C12E4 mixed reverse micelles by antisolvent CO₂, *Chem. Eur. J.* 8 (2002) 3879.
- [32] H.F. Zhang, J. Lu, B.X. Han, Precipitation of lysozyme solubilized in reverse micelles by dissolved CO₂, *J. Supercrit. Fluids* 20 (2001) 65.
- [33] J. Chen, J.L. Zhang, D.X. Liu, Z.M. Liu, B.X. Han, G.Y. Yang, Investigation on the precipitation, microenvironment and recovery of protein in CO₂-expanded reverse micellar solution, *J. Colloid Interface Sci. B: Biointerfaces* 33 (2004) 33.
- [34] V.N. Dorovskis-Taran, C. Veeger, A.J.W.G. Visser, Reverse micelles as a water-property-control system to investigate the hydration/activity relationship of α -chymotrypsin, *Eur. J. Biochem.* 218 (1993) 1013.
- [35] A.K. Singh, R.V. Aruna, Fluorescence studies of tryptophan and tryptophan-retinal Schiff base in reverse micellar matrix, *J. Photochem. Photobiol. A: Chem.* 89 (1995) 247.
- [36] D. Juminaga, W.J. Wedemeyer, R. Garduno-Juarez, M.A. Mc-Donald, H.A. Scheraga, Tyrosyl interactions in the folding and unfolding of bovine pancreatic ribonuclease A: a study of tyrosine-to-phenylalanine mutants, *Biochemistry* 36 (1997) 10131.
- [37] G. Panick, R. Winter, Pressure-induced unfolding/refolding of ribonuclease A: static and kinetic Fourier transform infrared spectroscopy study, *Biochemistry* 39 (2000) 1862.

- [38] T. Imoto, L.S. Forster, J.A. Rupley, F. Tanaka, Fluorescence of lysozyme: emissions from tryptophan residues 62 and 108 and energy migration, *Proc. Natl. Acad. Sci. U.S.A.* 69 (1972) 1151.
- [39] C. Petit, P. Brochette, M.P. Pileni, Hydrated electron in reverse micelles: 3. Distribution and location of probes such as ions and hydrophilic proteins, *J. Phys. Chem.* 90 (1986) 6517.
- [40] R.T. Raines, Ribonuclease A, *Chem. Rev.* 98 (1998) 1045.
- [41] K. Takeda, Y. Moriyama, From protein conformation in reverse micelle environment, in: *Encyclopedia of Surface and Colloid Science*, Dekker, 2004.
- [42] A. Chattopadhyay, S. Mukherjee, H. Raghuraman, Reverse micellar organization and dynamics: a wavelength-selective fluorescence approach, *J. Phys. Chem. B* 106 (2002) 13002.
- [43] G.W. Zhou, G.Z. Li, W.J. Chen, Fourier transform infrared investigation on water states and the conformations of aerosol-OT in reverse microemulsions, *Langmuir* 18 (2002) 4566.
- [44] J. Lu, B.X. Han, H.K. Yan, B. Bunsen-Ges, UV-vis spectroscopic study of molecular clustering in supercritical CO₂-acetone mixtures, *Ber. Bunsen-Ges. Phys. Chem. Chem. Phys.* 102 (1998) 695.
- [45] J.R. Lakowicz, S. Keating-Nakamoto, Red-edge excitation of fluorescence and dynamic properties of proteins and membranes, *Biochemistry* 23 (1984) 3013.
- [46] H. Kandori, Y. Yanszaki, J. Sasaki, R. Needleman, J.K. Lanyi, A. Maeda, *J. Am. Chem. Soc.* 117 (1995) 2118.
- [47] D. Haussinger, The role of cellular hydration in the regulation of cell function, *Biochem. J.* 313 (1996) 697.
- [48] S. Nishimura, H. Kandori, A. Maeda, Transmembrane signaling mediated by water in bovine rhodopsin, *Photochem. Photobiol.* 66 (1997) 796.
- [49] A. Chattopadhyay, S. Mukherjee, Red edge excitation shift of a deeply embedded membrane probe: implications in water penetration in the bilayer, *J. Phys. Chem. B* 103 (1999) 8180.
- [50] S.S. Rawat, S. Mukherjee, A. Chattopadhyay, Micellar organization and dynamics: a wavelength-selective fluorescence approach, *J. Phys. Chem. B* 101 (1997) 1922.
- [51] N.W. Fadnavis, Y. Chandraprakash, A. Deshpande, Protein-protein interactions in reverse micelles: trypsin shows superactivity towards a protein substrate α -chymotrypsinogen A in reverse micelles of sodium bis(2-ethylhexyl) sulfosuccinate (AOT) in isooctane, *Biochimie* 75 (1993) 995.
- [52] M. Wong, J.K. Thomas, M. Grätzel, Fluorescence probing of inverted micelles. The state of solubilized water clusters in alkane/diisooctyl sulfosuccinate (aerosol OT) solution, *J. Am. Chem. Soc.* 98 (1976) 2391.
- [53] B.A. Andrew, D.L. Pyle, J.A. Asenjo, The effects of pH and ionic-strength on the partitioning of 4 proteins in reverse micelle systems, *Biotechnol. Bioeng.* 43 (1994) 1052.